DOI: 10.1002/adsc.200700096

How does the Achiral Base Decide the Stereochemical Outcome in the Dynamic Kinetic Resolution of Sulfinyl Chlorides? A Computational Study

David Balcells,[a,b] Gregori Ujaque,[b] Inmaculada Fernández,[c] Noureddine Khiar,[d] and Feliu Maseras[a,b,*]

[a] Institute of Chemical Research of Catalonia (ICIQ), Av. Països Catalans 16, 43007 Tarragona, Catalonia, Spain
Fax: (+34)-977-920-231; e-mail: fmaseras@iciq.es
[b] Unitat de Química Física, Universitat Autònoma de Barcelona, Edifici Cn, 08193 Bellaterra, Catalonia, Spain
[c] Departamento de Química Orgánica y Farmacéutica, Facultad de Farmacia, Universidad de Sevilla, c/Profesor García González 2, 41012 Sevilla, Spain
[d] Instituto de Investigaciones Químicas, C.S.I.C-Universidad de Sevilla, c/Américo Vespucio, Isla de la Cartuja, 41092 Sevilla, Spain

Received: February 12, 2007; Revised: June 5, 2007; Published online: September 6, 2007

Supporting information for this article is available on the WWW under http://asc.wiley-vch.de/home/.

Abstract: The dynamic kinetic resolution of sulfinyl chlorides by addition of the optically active alcohol DAGOH (diacetone D-glucose) in the presence of non-chiral bases was theoretically studied at the ONIOM (Becke3LYP:UFF) level. The dependence of the stereochemical outcome on the nature of the base observed in this reaction was explored considering two electronically similar bases, pyridine and collidine, that are experimentally known to promote opposite diastereoselectivities. Our calculations reproduced the experimental result that the absolute configuration of sulfur in the major reaction product is *R* with pyridine but *S* with collidine. The analysis of the optimized geometries revealed that the most sterically active substituent around sulfur is the methyl of the substrate with pyridine but the base itself with collidine. This leads to an inversion of the chiral distribution of steric hindrance around sulfur that induces the reversal of the stereochemical outcome.

Keywords: asymmetric synthesis; chirality; diastereoselectivity; dynamic kinetic resolution; molecular modelling; nucleophilic substitution

Introduction

Chiral sulfoxides are compounds of high interest in organic chemistry due to their high optical stability,[1] and their wide use in asymmetric organic synthesis.[2,3] The total synthesis of several natural products, including steroids and alkaloids, has been performed using sulfoxides as chiral auxiliaries.[2] Furthermore, many biologically active compounds, like the antiulcer agent esomeprazole[4] and the anticancer drug sulforaphane,[5] contain chiral sulfinyl centers. Due to the interest in chiral sulfoxides, several synthetic methods have been developed in order to obtain these compounds.[3] The most important methods can be grouped into two families: the metal-catalyzed oxidation of prochiral sulfides, referred to as sulfoxidation, and the nucleophilic substitution on chiral sulfur derivatives. In most cases, sulfoxidation is performed using a peroxidic oxidant in combination with a chiral metal catalyst.[6,7] The nucleophilic substitution on chiral sulfur derivatives is especially efficient when dynamic kinetic resolution (DKR) is applied. Two relevant examples of this methodology are the *Cinchona*-assisted DKR[8–10] and the DAG synthetic method.[11–13]

In the DAG method (see Scheme 1), a racemate of a sulfinyl chloride is transformed into a chiral sulfi-

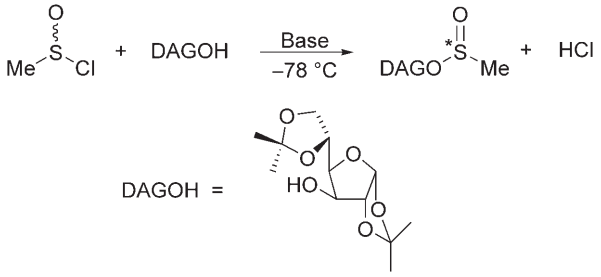

Scheme 1. The DAG synthetic method.

nate ester by dynamic kinetic resolution[14] using the DAGOH (diacetone D-glucose) chiral alcohol as resolving agent. The major diastereomer of the sulfinate ester is purified and the subsequent addition of a Grignard reagent gives rise to a chiral sulfoxide through the replacement of the ODAG substituent by an alkyl group. In most cases, this second reaction proceeds with very high yields and enantioselectivities through an S_N2 mechanism with total inversion of the sulfur configuration. Hence, the success of the DAG method is totally based on the yield and diastereoselectivity of the initial DKR step. The by-product of the DAGOH addition is HCl, which is neutralized with stoichiometric amounts of an organic base, like pyridine or triethylamine. The DAG method has been successfully used in the synthesis of C_2-symmetric bissulfoxides[12,13] that have been applied as chiral ligands in asymmetric synthesis.[15,16] Other compounds with pharmacological and synthetic[17] interest have been obtained by means of this method as well.

The DAG method is of particular interest due to the possibility of selecting the final absolute configuration of sulfur by changing the nature of the non chiral base, without any modification of DAGOH.[11–13] This interesting feature was found when the DAG method was initially tested in the synthesis of methanesulfinate esters[11] (see Table 1). Good yields and diastereoselectivities, up to 90% and 96% *de*, were obtained and the subsequent addition of Grignard reagents led to the formation of chiral sulfoxides with very high enantioselectivities (>98% *ee*). Interestingly, while the *R* configuration of the sulfinyl sulfur of $MeSO_2DAG$ (*RS*-diastereomer) was obtained with bases like pyridine or imidazole, the *SS*-diastereomer was the major reaction product when other bases like collidine or triethylamine were used. This unexpected dependence of the identity of the major diastereomer product on the nature of a cheap achiral assistant base is very useful. The traditional method of changing the stereochemical outcome of a process by reversing the absolute configuration of the chiral source would be indeed complicated in the DAG method. DAGOH is a chiral alcohol derived from natural and cheap D-glucose, while its enantiomer is very expensive. The method is certainly efficient, but it would be desirable to increase its selectivity and to extend its range of application. The design of more efficient systems is, however, severely hampered by the lack of mechanistic understanding of the origin of the diastereoselectivity reversal. The present work tries to solve this problem through theoretical calculations.

Table 1. Influence of the base on the stereochemical outcome of the DKR of methyl sulfinyl chloride by DAGOH.[11]

Base	(*R*/*S*)-$MeSO_2DAG$	% *de*
pyridine	93/7	86
DMAP[a]	78/22	56
imidazole	82/18	64
i-Pr_2NEt	2/98	96
collidine[b]	2/98	96
DMA[c]	37/63	26
NEt_3	2/98	96

[a] 4-*N*,*N*-Dimethylaminopyridine.
[b] 2,4,6-Trimethylpyridine.
[c] *N*,*N*-Dimethylaniline.

The mechanistic role of the base in the DAG method was clarified by us in two previous computational studies of this reaction.[18,19] Two chemical transformations are involved in the dynamic kinetic resolution of the sulfinyl chloride, namely the interconversion of both enantiomers of MeSOCl and the subsequent displacement of chlorine by DAGOH (see Scheme 2). Our theoretical studies showed that the base catalyzes the first process and assists the second one, reducing in both cases their energy barriers. The study on the chlorine displacement[19] revealed that the alcohol reacts directly with MeSOCl following an addition/elimination mechanism originally proposed by Bachrach.[20] The absolute configuration of sulfur is decided in the addition step, which involves a hydrogen transfer from the alcohol to the sulfinyl oxygen of the substrate. The base participates into the mecha-

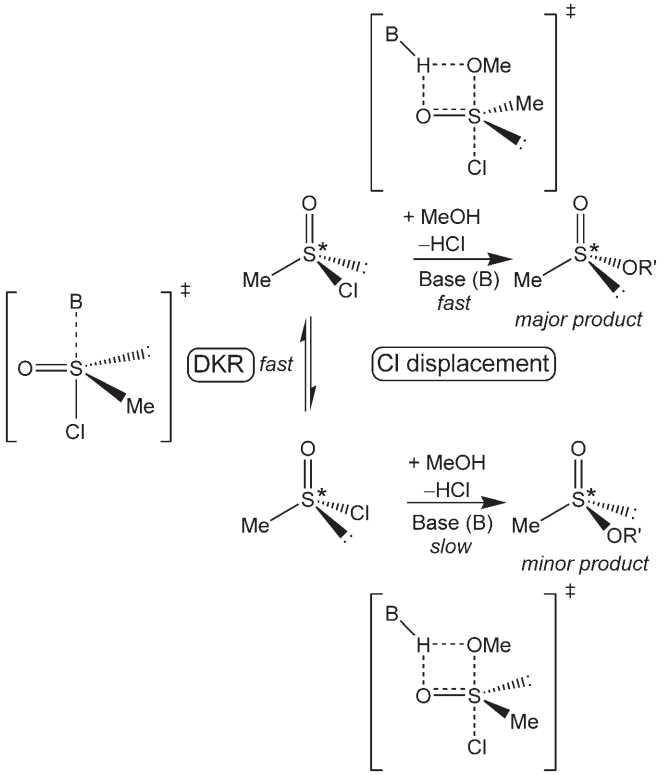

Scheme 2. Mechanistic scheme of the DAG method.

nism through the formation of a strong N–H bond with the transferred hydrogen.

In our previous studies, the reaction system was modelled replacing DAGOH by methanol[18,19] and the origin of the diastereoselectivity was thus not explored since all stereocenters of DAGOH were supressed. This question is tackled in the present study, in which the asymmetric addition of DAGOH to methanesulfinyl chloride is theoretically explored considering pyridine and collidine as bases. Interestingly, these two bases promoted opposite absolute configurations of sulfur in the reaction product,[11] in spite of their structural and electronic similarity (see Table 1). Several mechanisms and steps have been analyzed in our previous study of the model system.[19] The current work focuses on the addition step of the neutral mechanism, which is the rate-determining stereo-deciding step of the lowest energy path.

The theoretical study presented in this article was carried out using the ONIOM method.[21,22] Computational chemistry has been successfully applied to the study of organic synthetic methods,[23] including organocatalysis[24] and homogeneous catalysis.[25,26] Hybrid QM/MM methods are a valuable tool for the study of asymmetric reactions in which steric interactions play a prominent role,[27] and have been already used in several cases.[7,28–31]

Enantiomeric excesses were computed from the energy differences between the barriers of the lower energy paths leading to the *R* and *S* products.[32] Each transition state was labeled either P or C, depending on whether the base is pyridine or collidine respectively, followed by a TSR or TSS label, for the pro-*R* and pro-*S* transition states respectively, and a sequential number related with its relative energy. For instance, **P-TSR-2** is the second most stable pro-*R* transition state in the case of pyridine, and **C-TSS-1** is the most stable pro-*S* transition state with collidine.

Results

Pyridine-Assisted Addition of DAGOH

The kinetic resolution of methanesulfinyl chloride in the presence of DAGOH and pyridine was theoretically investigated. Our previous study revealed that the key step is the addition of DAGOH to MeSOCl which involves the trigonal bipyramid transition state represented in Figure 1. The consideration of the full DAGOH increases the structural complexity of the transition state. There are a variety of sources of conformational flexibility that give rise to a large conformational space. The first of them is associated to the absolute configuration around S, which is quantified by the Cl–S–O2–C1 dihedral angle, labeled as D1. Torsions around the unconstrained σ-bonds add to the

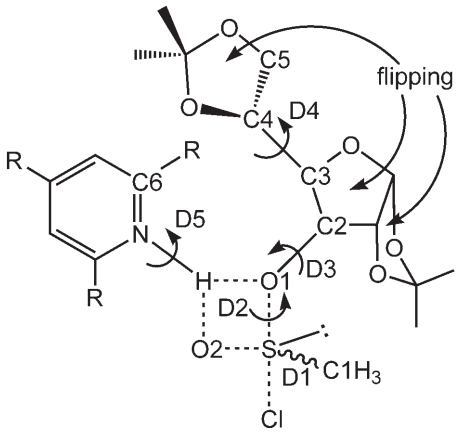

Figure 1. Sources of conformational flexibility in the addition transition state.

conformational complexity. There are four of these σ-bonds, labelled as D2, D3, D4 and D5 (see Figure 1), and rotation around them is quantified by the dihedral angles O2–S–O1–C2, S–O1–C2–C3, C2–C3–C4–C5 and O1–H–N–C6, respectively. There is finally the flexibility associated to the flipping of the three five-membered cycles of DAGOH.

The conformational analysis is further complicated by the correlation between the different sources of flexibility. Because of this, a systematic MCMM approach was adopted in order to sample the conformational space. This conformational search was performed for both the pro-*R* and pro-*S* transition states and the four most stable structures found in each case were reoptimized at the ONIOM level.

The optimized geometries of the most stable pro-*R* and pro-*S* transition states, labelled as **P-TSR-1** and **P-TSS-1** respectively, are presented in Figure 2. The values of all these geometrical parameters are very similar to those found in our study of the model system.[19] This similarity confirmed that these ONIOM transition states also correspond to the addition of DAGOH to MeSOCl coupled with a hydrogen transfer from O1 to O2 and the cleavage of the S-Cl bond. The dihedral angles (D1-5) and relative energies of all pro-*R* and pro-*S* transition states are collected in Table 2. Of course, D1 is negative in the pro-*R* transition states and positive in the pro-*S*, due to the inversion of the sulfur absolute configuration. Among the other values, it is worth mentioning D5. The values are closer to 0° than to 90°, especially in the lower energy structures, and this indicates that pyridine stays essentially coplanar with the H–O1–S–O2 plane.

The most stable transition state, **P-TSR-1**, leads to the formation of the *RS* diastereomer of the product in total agreement with the experimental results.[11] This saddle point is 1.0 kcal mol^{-1} more stable than **P-TSS-1**, which is the most stable pro-*S* transition state.

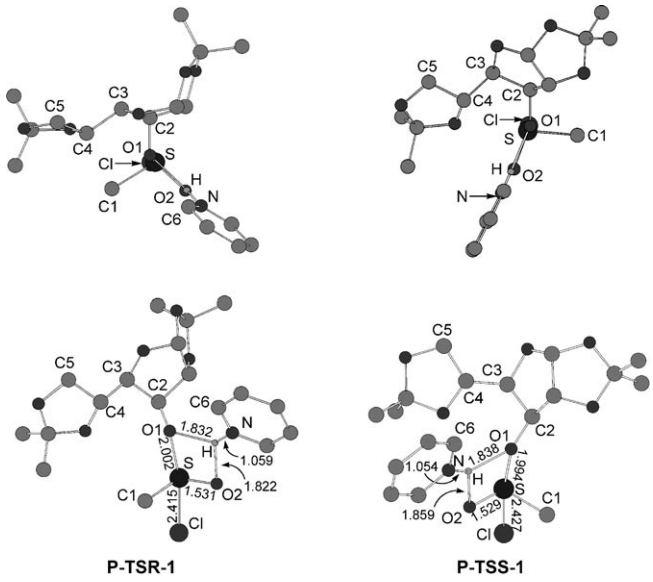

Figure 2. Top (*above*) and side (*below*) views of the most stable pro-*R* (left) and pro-*S* (right) transition states for the pyridine-assisted addition of DAGOH. All hydrogens, except the proton being transferred, were removed for clarity.

Table 2. Dihedral angles, in degrees, and relative energies, in kcal mol^{-1}, of the transition states corresponding to the pyridine-assisted addition of DAGOH. D1 = Cl–S–O2–C1, D2 = O2–S–O1–C2, D3 = S–O1–C2–C3, D4 = C2–C3–C4–C5, D5 = O1–H–N–C6.

TS	D1	D2	D3	D4	D5	E
P-TSR-1	−90.3	131.6	138.5	−176.1	11.6	0.0
P-TSR-2	−90.2	128.9	138.1	−171.1	10.3	0.4
P-TSR-3	−90.4	151.3	161.2	−54.6	21.1	2.7
P-TSR-4	−89.4	95.7	97.6	−78.0	48.4	4.3
P-TSS-1	90.3	−159.6	89.2	173.0	−3.0	1.0
P-TSS-2	90.4	−150.3	117.4	−168.0	−1.7	1.3
P-TSS-3	90.6	−162.9	86.9	177.2	−22.1	1.6
P-TSS-4	90.7	176.7	131.2	−59.1	−6.2	4.1

The preference for the pro-*R* pathway in the pyridine-assisted addition of DAGOH to MeSOCl can be rationalized comparing the **P-TSR-1** and **P-TSS-1** geometries. If we look at the top view of both geometries represented in the upper part of Figure 2, we can divide each structure in two fragments, namely DAG and the sulfur block, connected by the O1–C2 bond. Each fragment has two sterically active regions and the arrangement between them rules the relative energy of the structures. In the case of the sulfur block, the groups with potential steric activity are the C1-methyl (left side in **P-TSR-1**) and the base (right side in **P-TSR-1**). Their positions are inverted in **P-TSS-1**. The C1-methyl group happens to be more sterically active because the base, being coplanar with the H–O1–S–O2 plane, stays always away from DAGOH. DAGOH is constituted by two well differentiated molecular fragments linked by the C3–C4 bond: a bicycle consisting of two fused 5-membered cycles, that will be referred to as **C2,C3-BC**, and a single 5-membered cycle, that will be referred as **C4,C5-C**. The size and thus the steric bulk of **C2,C3-BC** is clearly larger than that of **C4,C5-C**. In both **P-TSR-1** and **P-TSS-1** the **C4,C5-C** and **C2,C3-BC** fragments of DAGOH are on the left and right sides of the H–O1–S–O2 plane, respectively. In contrast with this, due to the opposite configuration of sulfur, C1-methyl stands on the left in **P-TSR-1** but on the right in **P-TSS-1**. The lower stability of **P-TSS-1** in comparison with **P-TSR-1** can be thus associated with the steric repulsion between the C1-methyl and the bulkiest fragment of DAGOH, namely **C2,C3-BC**, in the former transition state. The structure **P-TSS-1** is in fact distorted with respect to the ideal arrangement around the Cl–S–O axis to reduce this steric interaction.

Collidine-Assisted Addition of DAGOH

The study presented above for pyridine was repeated with collidine. As in the case of pyridine, all sources of structural complexity, namely the two possible configurations of sulfur (D1), the rotation of four σ-bonds (D2-5) and the flipping of the cycles of DAGOH (see Figure 1), were considered. The conformational space was also inspected with a MCMM statistical approach and the four most stable pro-*R* and pro-*S* transition states were then recomputed at the ONIOM level.

The most stable pro-*R* and pro-*S* transition states, labeled as **C-TSR-1** and **C-TSS-1** respectively, are represented in Figure 3. As in the case of pyridine, the geometrical parameters of the reaction center are very similar in both structures and also similar to the values found in our previous study,[19] suggesting that these transition states also correspond to the addition of DAGOH to methanesulfinyl chloride. The relative energies and D1-5 dihedral angles of the most stable pro-*R* and pro-*S* transition states involving collidine as base are collected in Table 3.

A significant difference with respect to the case of pyridine is given by the dihedral angle D5, which measures the relative orientation of collidine with respect to the H–O1–S–O2 square plane. Pyridine is coplanar with this plane as shown by the values of D5 very close to 0° in all transition states (see Table 2). In contrast with this, the aromatic plane of collidine is clearly perpendicular to H1–O1–S–O2 as indicated by the absolute values of D5, close to 90° in all geometries. The different orientation of collidine in the addition transition state is due to the replacement of

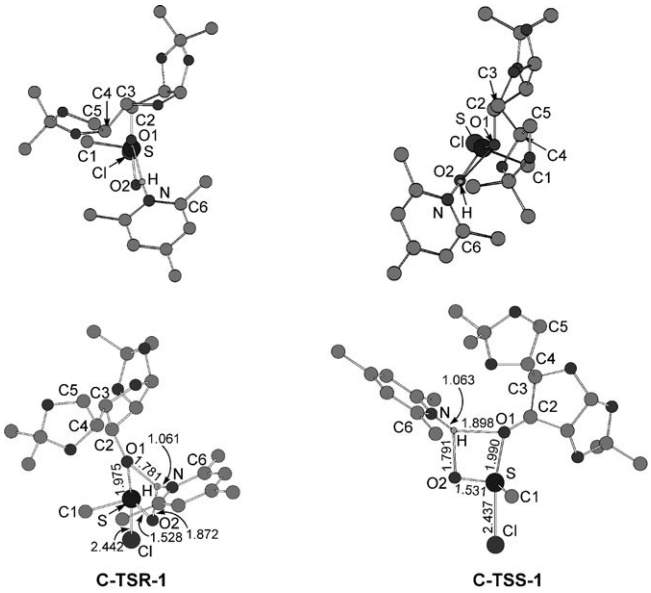

Figure 3. Top (*above*) and side (*below*) views of the most stable pro-*R* (left) and pro-*S* (right) transition states for the collidine-assisted addition of DAGOH. All hydrogens, except the proton being transferred, were removed for clarity.

Table 3. Dihedral angles, in degrees, and relative energies, in kcal mol^{-1}, of the transition states corresponding to the collidine-assisted addition of DAGOH. D1 = Cl–S–O2–C1, D2 = O2–S–O1–C2, D3 = S–O1–C2–C3, D4 = C2–C3–C4–C5, D5 = O1–H–N–C6.

TS	D1	D2	D3	D4	D5	E
C-TSR-1	−89.2	173.2	171.9	−168.2	−86.5	2.2
C-TSR-2	−90.2	158.9	160.6	−174.1	−101.2	2.3
C-TSR-3	−90.2	105.9	90.7	−84.9	−122.8	5.2
C-TSR-4	−92.5	145.6	172.0	−78.7	−119.9	9.6
C-TSS-1	89.9	−139.6	171.3	167.8	−88.9	0.0
C-TSS-2	89.9	−138.6	169.9	166.8	−91.5	0.1
C-TSS-3	89.6	−138.2	177.3	−176.3	−71.7	1.0
C-TSS-4	89.5	−136.4	−179.3	178.6	−78.8	1.3

the *ortho* hydrogens of pyridine by much bulkier methyl groups. The attractive CH···O interactions given by pyridine when D5 = 0° are consequently replaced by repulsive Me–O1 and Me–O2 steric interactions that are avoided with D5 = 90°. All attempts to optimize an addition transition state with D5 close to 0° failed. As will be explained below, this change in the relative orientation of the base is key for the diastereoselectivity reversal.

In contrast with the case of pyridine, the relative energies collected in Table 3 show that the most stable pro-*S* transition state, **C-TSS-1**, is favoured over the most stable pro-*R* transition state, **C-TSR-1**, by 2.2 kcal mol^{-1}. The preference for the pro-*S* pathway when the base is collidine can be rationalized comparing the optimized geometries of **C-TSR-1** and **C-TSS-1** (see Figure 3). Since the structure of DAG is the same regardless of the base used in the reaction, the steric model proposed for DAG in the pyridine-assisted addition should be exactly the same in the collidine-assisted pathway. As in the saddle points found for pyridine, while the **C4,C5-C** ring is on the left side of both the pro-*R* and pro-*S* transition states, the much bulkier **C2,C3-BC** bicycle is on the right side. Also as in **P-TSR-1** and **P-TSS-1** (see Figure 2), the inversion of sulfur implies that C1-methyl is on the left in the pro-*R* transition state and on the right in the pro-*S*. Nevertheless, with collidine the bulkiest fragment attached to sulfur is not the C1-methyl but instead the base attached to it across the rigid H1–O1–S–O2 plane. The non coplanar arrangement of collidine with respect to H–O1–S–O2 implies that the *ortho* methyls occupy the left and right sides of the H–O1–S–O2 plane pointing towards DAG. Thus, the critical interactions between DAG and the rest of the system will imply collidine instead of C1-methyl. The lower stability of **C-TSR-1** with respect to **C-TSS-1** is due to the close contact between collidine and **C2,C3-BC**, which are the bulkiest fragment around sulfur and the bulkiest part of DAG respectively.

Discussion

The relative energies found in the case of pyridine (see Table 2) showed that the most stable pro-*R* and pro-*S* transition states are **P-TSR-1** and **P-TSS-1**, respectively. Furthermore, **P-TSR-1** was more stable than **P-TSS-1** and thus the *RS*-diastereomer of the product should be the major reaction product, in total agreement with the experimental results (see Table 1). The energy gap between **P-TSR-1** and **P-TSS-1** is 1.0 kcal mol^{-1}, which corresponds to a theoretical diastereomeric excess at −78 °C of 85 % *de*, very close to the experimental value of 86 % *de*. In the case of collidine, the relative energies collected in Table 3 showed that the most stable pro-*S* transition state, **C-TSS-1**, is favoured over the most stable pro-*R* transition state, **C-TSR-1**, by 2.2 kcal mol^{-1}. This energy gap implies a theoretical diastereomeric excess of 99 % *de*, which is quite close to the experimental value (96 % *de*). Hence, the theoretical model predicts that the diastereoselectivity reached with collidine is slightly better than that obtained with pyridine. Nevertheless, the important result is that the calculations reproduced the most relevant feature of the DAG asymmetric method, namely the diastereoselectivity reversal induced by the nature of the base. Our results showed that while the preferred reaction pathway is the pro-*R* when the base is pyridine, with colli-

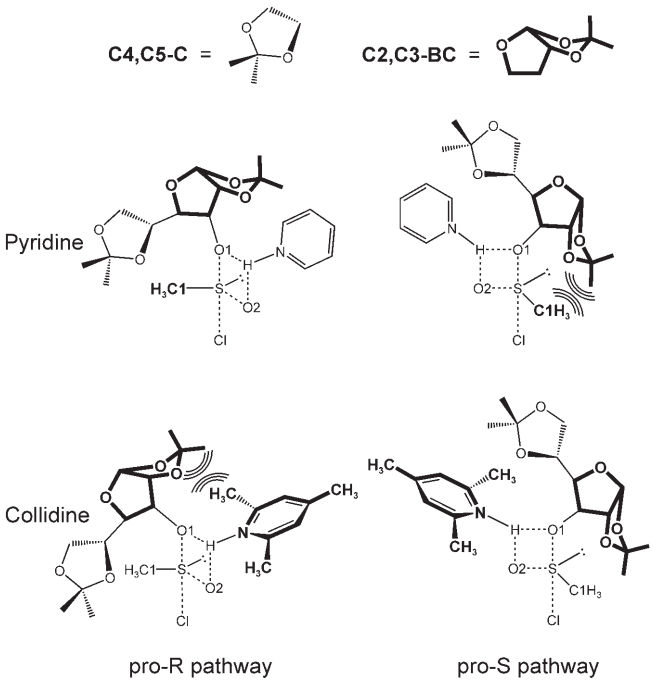

Figure 4. Origin of the diastereoselectivity reversal in the DAG method.

dine the fastest addition corresponds to the pro-*S* pathway. This diastereoselectivity reversal can be rationalized comparing the structures and relative energies of the most stable pro-*R* and pro-*S* transition states found for each base.

Our calculations showed that the addition transition state has a trigonal bipyramid geometry in which DAGOH and Cl occupy the axial positions. The other fragments attached to sulfur lie on the equatorial plane of the molecule. These fragments are C1-methyl and O2 which are in *cis* position, and thus in close proximity, with respect to DAGOH. The OH group of DAGOH is directly involved in the H–O1–S–O2 reaction center. The rest of the molecule (DAG) discriminates the pro-*R* and pro-*S* pathways through diastereomeric interactions with the groups attached to sulfur (see Figure 4). The axial position of Cl is fixed since the O1-*trans*-Cl arrangement is an electronic requirement of the addition process. Hence, the two possible chiral environments around sulfur are associated to the relative positions of C1-methyl and O2 on the equatorial plane.

DAG is able to recognize and differentiate these two configurations thanks to its chiral structure which is clearly divided in two parts that introduce different degrees of steric hindrance. These two parts are the **C4,C5-C** cycle and the much bulkier **C2,C3-BC** bicycle. In all transition states, DAGOH occupies both sides of the H–O1–S–O2 plane in such a manner that **C2,C3-BC** and **C4,C5-C** are always on the right and left sides of this plane respectively. Hence, the preferred diastereomeric pathway will be that one having the less bulky substituent of the sulfur block in the right side. This substituent is O2 with pyridine since the whole Base-H–O1–S–O2 set of atoms is in a coplanar arrangement in which the base stands far from DAGOH. With collidine, the Base-H–O1–S–O2 fragment becomes the bulkiest substituent due to the alkylation and subsequent rotation of the base. Therefore, with pyridine the most stable transition state is that with O2 on the right side while for collidine is that with O2 on the left side, and obviously while the former transition state leads to the *RS*-diastereomer, the latter gives rise to the *SS*-diastereomer. In summary, our results revealed that the replacement of pyridine by collidine induced a reversal of diastereoselectivity due to an inversion of the chiral distribution of steric bulk around sulfur.

Conclusions

Our computational study at the ONIOM (B3LYP:UFF) level on the dynamic kinetic resolution of methyl sulfinyl chloride by DAGOH in the presence of organic bases reproduces the unusual experimental behavior and provides a rational explanation of the reversal in diastereoselectivity induced by the nature of the base. The opposite sense of diastereoselection given by two very similar bases was successfully reproduced, with the pyridine system leading to the *R* product and the collidine system producing the *S* product.

The analysis of the results obtained for the pyridine-assisted addition showed that the lowest energy pathway was pro-*R*, due to a favourable match between the bulkiest part of DAGOH (**C2,C3-BC**) and the base. In this case, pyridine stands coplanar with the reaction center and does not play any relevant steric role. The pro-*S* transition state has a higher energy because of the presence of repulsive interactions between the methyl attached to sulfur (C1-methyl) and **C2,C3-BC**.

In the collidine-assisted addition the less stable transition state was pro-*R* because of repulsive interactions between the base and **C2,C3-BC**. In this case, collidine stands perpendicular to the planar reaction center, due to the presence of methyl groups in the *ortho*-N positions, and becomes the most sterically active fragment around sulfur. Since the base and C1-methyl occupy opposite sides of the transition state that are exchanged by the inversion of sulfur, the reversal of the steric role of these substituents, associated with the change of the base, induces the inversion of the diastereoselectivity.

Our computational study has been limited to two particular bases, pyridine and collidine, but the resulting model is likely to have a general applicability on

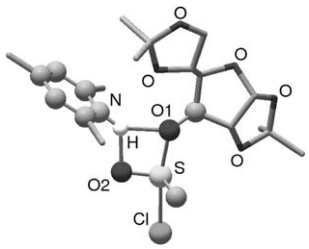

Figure 5. ONIOM QM (ball and stick) and MM (tube) partitions in the case of collidine.

the effect of the base on the stereochemical outcome of the DAG method. Available experimental data indicate that it is always the bulkier bases, with an sp^3 nitrogen or a sterically demanding sp^2 nitrogen, that favor the *SS*-diastereomer, while the less sterically demanding bases like pyridine and its close derivatives favor the *RS*-diastereomer.

Experimental Section

The present theoretical study was carried out using the ONIOM method[21,22] as implemented in Gaussian03.[33] This hybrid QM/MM method was applied by dividing the system in two parts. One of these parts was computed at a high quantum mechanical level (QM part) and the other was computed with a molecular mechanics method (MM part). In the QM calculation, the dangling bonds associated to the QM-MM interface were capped with hydrogens. The particular QM/MM partition adopted in our study is represented in Figure 5 for the case of collidine. The QM part is analogous to the system considered in our previous computational studies, in which DAGOH was modelled as methanol.[18,19] The rest of the DAGOH structure is included in the MM part together with the three methyl groups of collidine. The full base is included in the QM part in the case of pyridine. All calculations were done at the ONIOM (Becke3LYP:UFF) level, *i.e.*, the QM part was computed with the hybrid Becke3LYP density functional[34,35] and the MM part was computed using the UFF force field.[36]

The 6–31G(d) basis set[37,38] was used in the QM calculations to describe nitrogen, oxygen, carbon and hydrogen. In the case of sulfur and chlorine, the ten innermost electrons were replaced with an effective core potential.[39] The valence double-ζ basis set associated to the pseudopotential in the program,[33] with the contraction labelled as LANL2DZ, was used for these two elements and supplemented with d functions.[40] All elements involved in the system were thus described with a double-ζ quality basis set including polarization *d* functions. The suitability of this basis set was confirmed by us in a previous study.[18]

The geometry optimizations were full except for the link bonds. All energies given in the text are relative potential energies in gas phase. Diastereomeric excesses were computed assuming that the relative population of the *R* and *S* products is given by the Maxwell–Boltzmann distribution of the energies of the associated transition states at the temperature in which the experiments were performed (−78 °C). The nature of the transition states was not confirmed computing the frequencies. Nevertheless, in all cases the arrangement of the atoms involved in the reaction center was very similar to that found in our previous model study,[19] in which the transition states were characterized by vibrational analysis and IRC calculations.

The large conformational space of the system was systematically explored using the MCMM (Monte Carlo Multiple Minimum) approach[41,42] as implemented in the MacroModel 8.5 program[43] The potential energy was computed with the MMFF94 force field.[44] The model transition state found in our previous study[19] was modified replacing OMe by ODAG and considering either pyridine or collidine as bases. The conformational space was scanned taking into account all possible bond rotations (see Figure 1) and keeping the transition vector (S−O1, S−O2, O1−H, O2−H, N−H and S−Cl distances) frozen. For both the pro-*R* and pro-*S* pathways, the four most stable conformations found in the MCMM search were fully reoptimized at the ONIOM (Becke3LYP:UFF) level.

Acknowledgements

Financial support from the ICIQ foundation and the Spanish MEC through Projects CTQ2005–09000-CO1–02, CTQ2005–09000-CO1–01, BQU2003–00937 and Consolider Ingenio 2010 CSD2006–0003 and from the Catalan DURSI through projects 2005SGR00715 and 2005SGR00896. G.U. acknowledges the Spanish MEC for a "Ramón y Cajal" contract.

References

[1] D. R. Rayner, A. J. Gordon, K. Mislow, *J. Am. Chem. Soc.* **1968**, *90,* 4854.
[2] M. C. Carreño, *Chem. Rev.* **1995**, 1717.
[3] I. Fernández, N. Khiar, *Chem. Rev.* **2003**, *103,* 3651.
[4] J. Renfrey, S. Featherstone, *Nature Rev. Drug Discov.* **2002**, *1,* 175.
[5] T. J. Brown, R. F. Chapman, D. C. Cook, T. W. Hart, I. M. McLay, R. Jordan, J. S. Mason, M. N. Palfreyman, R. J. A. Walsh, M. T. Withnall, J.-C. Aloup, I. Cavero, F. D. , C. James, S. Mondot, *J. Med. Chem.* **1992**, *35,* 3613.
[6] J. Legros, C. Bolm, *Angew. Chem. Int. Ed. Engl.* **2004**, *43,* 4225.
[7] D. Balcells, F. Maseras, G. Ujaque, *J. Am. Chem. Soc.* **2005**, *127,* 3624.
[8] J. W. Evans, M. B. Fierman, S. J. Miller, J. A. Ellman, *J. Am. Chem. Soc.* **2004**, *126,* 8134.
[9] J. W. Evans, M. B. Fierman, S. J. Miller, J. A. Ellman, *Org. Lett.* **2005**, *7,* 1733.
[10] N. Shibata, M. Matsunaga, M. Nakagawa, T. Fukuzumi, S. Nakamura, T. Toru, *J. Am. Chem. Soc.* **2005**, *127,* 1374.
[11] I. Fernández, N. Khiar, J. M. Llera, F. Alcudia, *J. Org. Chem.* **1992**, *57,* 6789.
[12] N. Khiar, F. Alcudia, J. Espartero, L. Rodríguez, I. Fernández, *J. Am. Chem. Soc.* **2000**, *122,* 7598.

[13] N. Khiar, C. S. Araujo, F. Alcudia, I. Fernández, *J. Org. Chem.* **2002**, *67,* 345.
[14] S. Caddick, K. Jenkins, *Chem. Soc., Rev.* **1996**, 447.
[15] N. Khiar, I. Fernández, F. Alcudia, *Tetrahedron Lett.* **1993**, *34,* 123.
[16] R. Tokunoh, M. Sodeoka, K. Aoe, M. Shibasaki, *Tetrahedron Lett.* **1995**, *44,* 8035.
[17] M. C. Carreño, J. L. García-Ruano, M. C. Maestro, L. M. Martín Cabrejas, *Tetrahedron: Asymmetry* **1993**, *4,* 727.
[18] D. Balcells, F. Maseras, N. Khiar, *Org. Lett.* **2004**, *6,* 2197.
[19] D. Balcells, G. Ujaque, I. Fernandez, N. Khiar, F. Maseras, *J. Org. Chem.* **2006**, *71*, 6388.
[20] S. H. Norton, S. M. Bachrach, J. M. Hayes, *J. Org. Chem.* **2005**, *70,* 5896.
[21] F. Maseras, K. Morokuma, *J. Comput. Chem.* **1995**, *16,* 1170.
[22] S. Dapprich, I. Komaromi, K. S. Byun, K. Morokuma, M. Frisch, *J. Mol. Struct. (THEOCHEM)* **1999**, *461–462,* 1.
[23] J. Dolbier W. R. , H. Koroniak, K. N. Houk, C. Sheu, *Acc. Chem. Res.* **1996**, *29,* 471.
[24] C. Allemann, R. Gordillo, F. R. Clemente, P. H.-Y. Cheong, K. N. Houk, *Acc. Chem. Res.* **2004**, *37,* 558.
[25] T. Ziegler, J. Autschbach, *Chem. Rev.* **2005**, *105,* 2695.
[26] *Computational Modeling of Homogeneous Catalysis*, (Eds.: F. Maseras, A. Lledós), Kluwer, Dordrecht, **2002**.
[27] G. Ujaque, F. Maseras, *Struct. Bond.* **2004**, *112,* 117.
[28] G. Ujaque, F. Maseras, A. Lledós, *J. Am. Chem. Soc.* **1999**, *121,* 1317.
[29] S. Feldgus, C. R. Landis, *J. Am. Chem. Soc.* **2000**, *122,* 12714.
[30] A. M. Segarra, E. Daura-Oller, C. Claver, J. M. Poblet, C. Bo, E. Fernández, *Chem. Eur. J.* **2004**, *10*, 6456.
[31] S. Mori, T. Vreven, K. Morokuma, *Chem. Asian J.* **2006**, *1*, 391.
[32] D. Balcells, F. Maseras, *New J. Chem.* **2007**, *31*, 333.
[33] M. J. Frisch, M. G. W. Trucks, H. B. Schlegel, G. E. Scuseria, M. A. Robb, J. R. Cheeseman, J. A. Montgomery, Jr., T. Vreven, K. N. Kudin, J. C. Burant, J. M. Millam, S. S. Iyengar, J. Tomasi, V. Barone, B. Mennucci, M. Cossi, G. Scalmani, N. Rega, G. A. Petersson, H. Nakatsuji, M. Hada, M. Ehara, K. Toyota, R. Fukuda, J. Hasegawa, M. Ishida, T. Nakajima, Y. Honda, O. Kitao, H. Nakai, M. Klene, X. Li, J. E. Knox, H. P. Hratchian, J. B. Cross, V. Bakken, C. Adamo, J. Jaramillo, R. Gomperts, R. E. Stratmann, O. Yazyev, A. J. Austin, R. Cammi, C. Pomelli, J. W. Ochterski, P. Y. Ayala, K. Morokuma, G. A. Voth, P. Salvador, J. J. Dannenberg, V. G. Zakrzewski, S. Dapprich, A. D. Daniels, M. C. Strain, O. Farkas, D. K. Malick, A. D. Rabuck, K. Raghavachari, J. B. Foresman, J. V. Ortiz, Q. Cui, A. G. Baboul, S. Clifford, J. Cioslowski, B. B. Stefanov, G. Liu, A. Liashenko, P. Piskorz, I. Komaromi, R. L. Martin, D. J. Fox, T. Keith, M. A. Al-Laham, C. Y. Peng, A. Nanayakkara, M. Challacombe, P. M. W. Gill, B. Johnson, W. Chen, M. W. Wong, C. Gonzalez, J. A. Pople, *Gaussian03*, Gaussian, Inc., Wallingford, CT, **2004**.
[34] A. D. Becke, *J. Chem. Phys.* **1993**, *98,* 5648.
[35] C. Lee, R. G. Parr, W. Yang, *Phys. Rev.* **1988**, *37,* B785.
[36] A. K. Rappé, C. J. Casewit, D. S. Colwell, W. A. Goddard, W. N. Skiff, *J. Am. Chem. Soc.* **1992**, *114,* 10024.
[37] W. J. Hehre, R. Ditchfield, J. A. Pople, *J. Phys. Chem.* **1972**, *56,* 2257.
[38] P. C. Hariharan, J. A. Pople, *Theor. Chim. Acta* **1973**, *28,* 213.
[39] W. R. Wadt, P. J. Hay, *J. Chem. Phys.* **1985**, *82,* 284.
[40] A. Höllwarth, M. Böhme, S. Dapprich, A. W. Ehlers, A. Gobbi, V. Jonas, K. F. Köhler, R. Stegmann, A. Veldkamp, G. Frenking, *Chem. Phys. Lett.* **1993**, *208,* 237.
[41] G. Chang, W. C. Guida, W. C. Still, *J. Am. Chem. Soc.* **1989**, *111,* 4379.
[42] M. Saunders, K. N. Houk, Y. D. Wu, W. C. Still, M. Lipton, G. Chang, W. C. Guida, *J. Am. Chem. Soc.* **1990**, *112,* 1419.
[43] MacroModel 8.5, Schrödinger L.L.C., **2003**.
[44] T. A. Halgren *J. Comput. Chem.* **1999**, *20,* 720.

